ADVANCED PHOTONICS RESEARCH
Open Access
www.adpr-journal.com

Pixelated Photonic Crystals

Urban Mur and Miha Ravnik*

Photonic crystals can prevent or allow light of certain frequencies to propagate in distinct directions in anomalous and useful ways for use as waveguides, laser cavities, and topological light propagation. However, there exist limited approaches for fundamental reconfiguration of photonic crystals, such as changing the unit cell to various and on-demand geometries and symmetries. This work introduces the concept of pixelated 2D photonic crystals where the variability of the dielectric profile is achieved by a pixelated matrix of the material. Specifically, the cross sections of dielectric cylindrical pillars distributed in a photonic crystal lattice are replaced with pixelated circles using different resolutions and the corresponding band diagrams are calculated. The comparison to the band diagrams of the original structure shows that the original—and today typically used—cylindrical design can be well approximated by as few as 5×5 square switchable pixels while retaining less than 1% change in the photonic band structure. Experimental realization of switchable pixelation is proposed based on the liquid crystal display (LCD) technology with high birefringence materials. More generally, the demonstrated approach to reconfigurable 2D photonic crystal based on switchable pixels can enable realization of diverse fundamentally reconfigurable advanced optical materials.

1. Introduction

Photonic crystals are low-loss periodic dielectric media[1] that are constructed of material components with different dielectric constants and arranged into different subwavelength structures, such as slabs,[2] pillars,[1] spheres,[3] gyroids,[4] and other. If the dielectric constants of the materials in the photonic crystals are sufficiently different and if the absorption is minimal, then the refraction and reflection from all the possible effective interfaces between different material components produce interesting phenomena for photons, including selective light diffraction,[5] waveguiding,[6] lasing,[7] and topologically protected phenomena.[8] Photonic crystals are composed of fixed periodic subwavelength structures, which determine their band structure. Once the photonic crystal is produced, the band structure can be tuned by controlling the refractive index of the elements or their surroundings[9–14] by changing the optical properties of the material with nonlinear material's response,[15] using phase changing materials,[16,17] applying mechanical stress,[18,19] or changing temperature.[20] Nevertheless, reconfiguring the geometry and symmetry of the unit cells of the photonic crystals beyond the tuning of the operational frequencies remains a challenge.

Many optical applications are based on pixels—picture elements—as the isolated entities of larger planar structures. Examples include detector[21] and light-emitting diode (LED) arrays and metasurfaces.[22] Pixelated design is often combined with liquid crystals (LCs) where LC orientation is manipulated separately in each pixel by external electromagnetic fields in order to modulate the transmission of light by changing the polarization-dependent refractive index of the material. LC-based devices include spatial light modulators,[23,24] liquid crystal on silicon (LCOS) displays,[25,26] and widely used liquid crystal displays (LCDs). In addition to display technology, LCD technical solutions were recently transferred to applications like particle transport[27] and LCD 3D printing,[28,29] where the display acts as a mask.

In this article, we demonstrate how pixelation of the unit cell can be developed to realize fundamentally tunable 2D photonic crystals, including their band structure. The goal is to explore whether the dielectric structures in the unit cell of the photonic crystal could be constructed of pixels. Such design would allow for simplified engineering and more robust construction of photonic crystals. As a route toward experimental realization, we discuss the use of LCD technology for constructing reconfigurable photonic crystals by switching (effective) refractive index in each pixel separately.

2. Results

A typical design of 2D photonic crystal consists of a square lattice of cylindrical dielectric columns in vacuum, which are homogeneous in the z direction and imagined to be infinitely tall. For a certain selection of parameters, namely, ratio between the

U. Mur, M. Ravnik
Faculty of Mathematics and Physics
University of Ljubljana
Jadranska cesta 19, 1000 Ljubljana, Slovenia
E-mail: urban.mur@fmf.uni-lj.si

M. Ravnik
Condensed Matter Physics Department
Josef Stefan Institute
Jamova cesta 39, 1000 Ljubljana, Slovenia

The ORCID identification number(s) for the author(s) of this article can be found under https://doi.org/10.1002/adpr.202300082.

© 2023 The Authors. Advanced Photonics Research published by Wiley-VCH GmbH. This is an open access article under the terms of the Creative Commons Attribution License, which permits use, distribution and reproduction in any medium, provided the original work is properly cited.

DOI: 10.1002/adpr.202300082

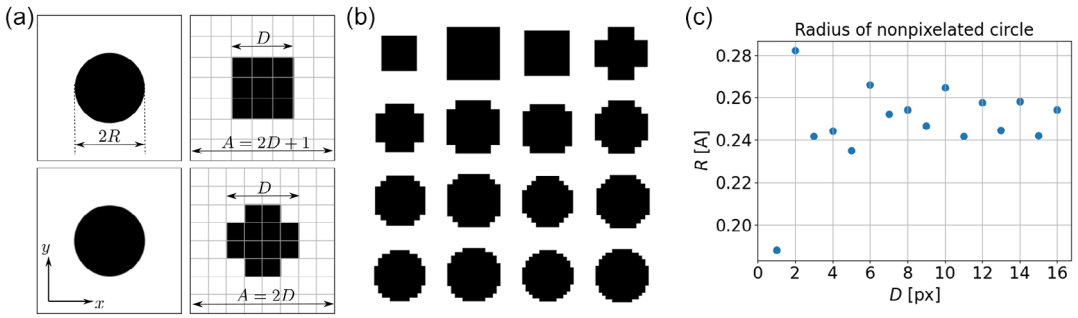

Figure 1. Design of pixelated approximations of 2D photonic crystal made of dielectric cylindrical columns. a) A circular cross section of a column with the radius R is approximated by pixels. The unit cell size A in units of pixels is determined by different formulas for even and odd diameter of the pixelated column D, as shown by Equation (1); b) Pixelated approximations of a circular cross section for $D = (1, \ldots, 16)$; and c) Radius of the circular column with the same area as its pixelated approximation in the units of unit cell size A, as defined by Equation (2).

column radius and the unit cell size for given dielectric contrast, full bandgaps are observed for in-plane ($k_z = 0$) propagation of transverse magnetic (TM) modes with $\vec{E} = (0, 0, E_z)$ and $\vec{H} = (H_x, H_y, 0)$. Here, we will analyze the effects of rough pixelation of the columns on the band structure and bandgaps of the photonic crystal.

The unit cell of such photonic crystal has a shape of a square with a cylindrical column placed in the middle, as shown in **Figure 1**a. In order to analyze the effects of pixilation, we approximate the cross section of the column by an array of squared pixels with the diameter D of the pixelated circle ranging from 1 to 16 pixels, as shown in Figure 1a. "Full" pixels in black represent the dielectric material with $\varepsilon = 12$ and "empty" pixels in white the surrounding, here vacuum with $\varepsilon = 1$. The best approximations of the circular cross section of a cylinder for each D are determined by minimizing the polar second moment of the array, as described in ref.[30] with the constraint to respect the mirror symmetries of the square. The arrays used in calculations are shown in Figure 1b. In order to ensure symmetrical placing of the pixelated array in the middle of the unit cell, the lattice constant A in the units of pixels is determined by the following formula

$$A = \begin{cases} 2D & D \text{ is even} \\ 2D + 1 & D \text{ is odd} \end{cases} \tag{1}$$

which allows to place $D/2$ empty pixels for even D and $(D + 1)/2$ empty pixels for odd D symmetrically on each side of the array (see Figure 1a). Band structures of pixelated approximations are compared to the band structures of the cylindrical columns with the same area—i.e., same amount of dielectric material in the unit cell. Radius of cylindrical column, measured in the units of the lattice constant A, is determined as

$$R = \sqrt{\frac{N}{\pi^2}} \tag{2}$$

where N is the number of full pixels in the array. Figure 1c shows how R depends on D for selected pixelated arrays and converges

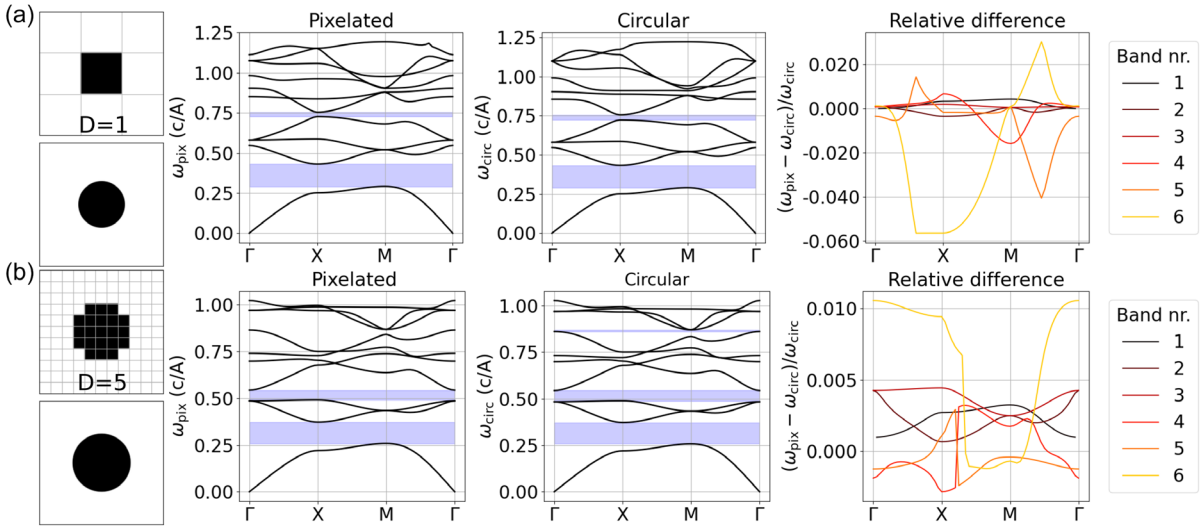

Figure 2. Comparison of band diagrams of a square lattice of cylindrical dielectric columns with circular cross sections and their pixelated approximations for a) $D = 1$ and b) $D = 5$. Areas of dielectric materials in the unit cell are matched. Far right plots show the relative difference between the band diagrams.

© 2023 The Authors. Advanced Photonics Research published by Wiley-VCH GmbH

toward $R = 0.25A$. The even–odd effect, showing in larger R for even D, occurs due to additional pixel being added to the surrounding for odd D in Equation (1), to ensure that the unit cell preserves symmetries of a square (see Figure 1a). Alternatively, a pixel could be subtracted, leading to the opposite effect, but same conclusions. Numerical calculations were performed by using MIT Photonic Bands (MPB) software package.[31] The resolution in calculations was 200 grid points per unit cell in each direction and was slightly adjusted for each D so that each pixel in the array consisted of the integer number of grid points and no additional interpolation was needed.

Band diagrams for photonic crystals consisting of pixelated and circular columns for $D = 1$ and $D = 5$ are shown in **Figure 2**. Surprisingly, already for $D = 1$ (Figure 2a), where circle is approximated by a square, a good agreement in terms of band diagrams is achieved. In fact, there are no distinguishable differences between the two for the first four bands, which lay beneath the second bandgap, marked with blue shades. To quantify that, we plot the relative difference between the frequencies of the bands in both diagrams $(\omega^{(\mathrm{pix})} - \omega^{(\mathrm{circ})})/\omega^{(\mathrm{circ})}$. The results show that the relative difference in frequency is in the range of 1% for the bands below the second bandgap and even below 0.5% for the first three bands, regardless of the direction of propagation. The difference gets gradually larger for higher bands. Similar results are obtained for $D = 5$, where relative differences for first four bands stay in the range of 0.5%; however also matching of higher bands is improved, namely, relative difference for bands 5 and 6 in this case also drops below 1%. Importantly, for $D = 5$, only three bands lay beneath the second gap, compared to four for $D = 1$. The reason is considerably smaller amount of dielectric material in the unit cell for $D = 1$, which can also be seen from $R(D)$ plot in Figure 1c. For every $D > 1$, the number of bands below the second gap is 3.

Next, we analyze the positions and sizes of first two full bandgaps in the system. The results are shown in **Figure 3** and **4**. Position of bandgap is determined by its central (midgap) frequency, which is calculated as the average of the upper and lower limit frequency. Positions of bandgaps for different values of D are shown in Figure 3a. Once again, we observe that $D = 1$ is a standout due to lower amount of dielectric material in a unit cell. Similarly, the reason why for odd D bandgaps systematically occur at slightly higher frequencies than for even D is that the radius of the associated cylindrical column is systematically smaller for odd D as shown in Figure 1c. In Figure 3b, relative differences of midgap frequencies $(\omega_{\mathrm{mid}}^{(\mathrm{pix})} - \omega_{\mathrm{mid}}^{(\mathrm{circ})})/\omega_{\mathrm{mid}}^{(\mathrm{circ})}$ between pixelated and cylindrical column are shown. Remarkably, positions of both bandgaps are similar in pixelated and cylindrical case with the difference being smaller than the 1%.

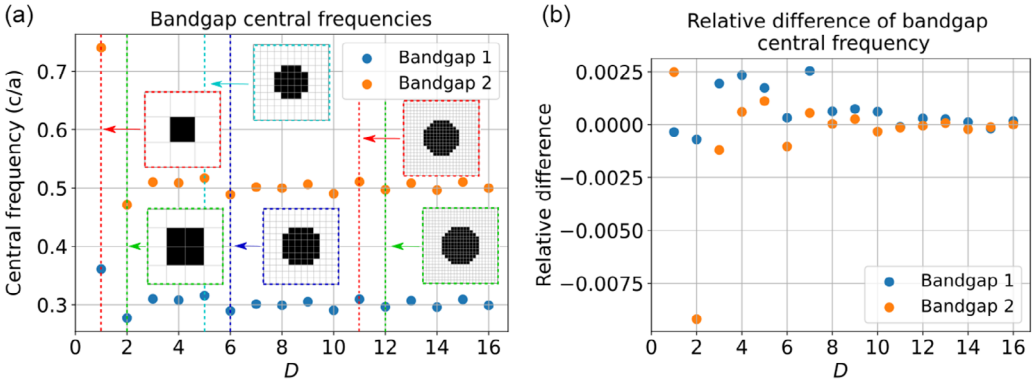

Figure 3. Bandgap positions in the band diagrams of pixelated cylindrical columns. a) Midgap frequencies of the first two bandgaps for different values of D. Insets show unit cells of pixelated cylindrical columns for a few selected values of D; and b) Relative difference of the frequency in the middle of the gap of pixelated columns, compared to the frequency in the middle of the same bandgap in the diagram of circular pillars.

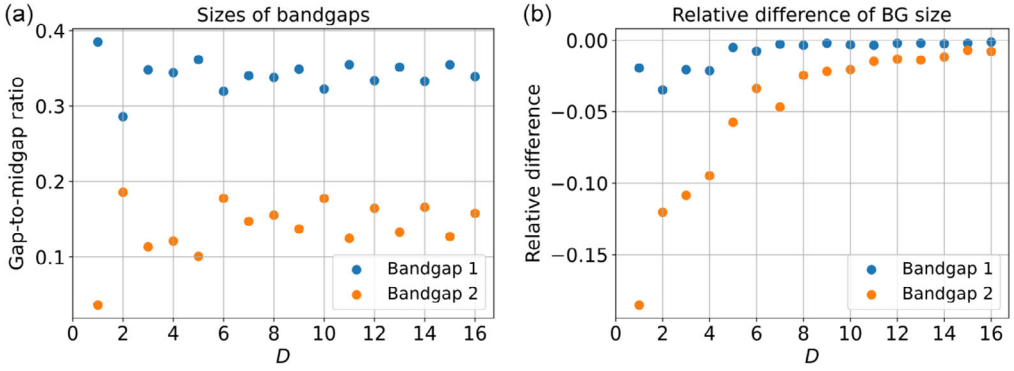

Figure 4. Sizes of first two bandgaps in the band diagrams of pixelated cylindrical columns. a) Gap–midgap ratio of the first two bandgaps for different values of D; and b) Relative difference of the bandgap size, compared to the size of the same bandgap in the diagram of circular pillars.

© 2023 The Authors. Advanced Photonics Research published by Wiley-VCH GmbH

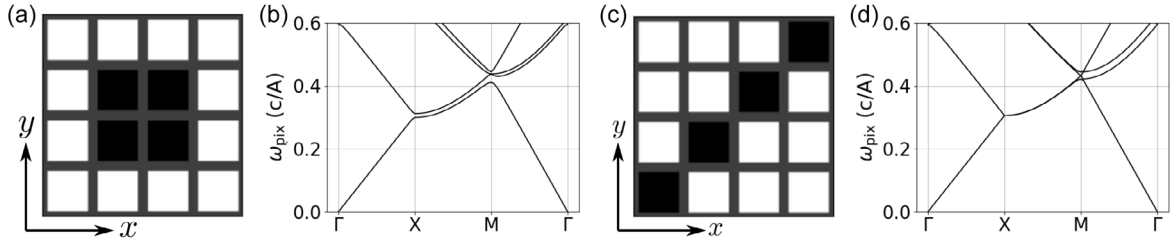

Figure 5. Possible experimental realization of a 2D pixelated photonic crystal, based on LCs. a) The unit cell is composed of 4×4 LC pixels, with the size of $D \times D$, separated by dielectric shield walls ($\varepsilon_{\text{wall}} = 3$), with the thickness of $0.2D$, shown in gray. Black pixels represent the out-of-plane LC orientation with effective refractive index of $n_e^2 = \varepsilon_e = 3.24$ for TM polarization, and white pixels represent the in-plane LC orientation with the effective refractive index of $n_o^2 = \varepsilon_o = 2.25$ for TM polarization; b) Corresponding band diagram. A local bandgap with the gap-to-midgap ratio of 0.06 occurs at the M point and has the midgap frequency of $0.423c/A$; c) Unit cell with a different distribution of "empty" and "full" pixels; and d) corresponding band diagram.

Sizes of bandgaps are shown in Figure 4a in terms of gap–midgap ratios. Again, we can notice that the sizes of bandgaps directly reflect the radius of the cylinders. Relative differences of bandgap sizes are shown in Figure 4b. First, we notice that the relative difference in bandgap size is considerably larger than the relative difference in bandgap position. For the first bandgap, the reason for this is that the frequency of the first band in point M, which determines the lower end of the gap is in general larger for pixelated case than cylindrical. Oppositely, the frequency of the second band in point X, which determines the upper end of the gap, is lower for the pixelated case. The gap is therefore effectively shrunken. For the second gap, the first reason is simply lower accuracy for higher bands and also that the gap is relatively thinner, meaning that the same absolute difference in band frequencies will lead to larger relative changes in sizes.

In the calculations presented so far, the dielectric contrast between the pillar and the surrounding was rather high ($\Delta\varepsilon = 11$), compared to the contrasts between the ordinary (n_o) and extraordinary (n_e) refractive index—the birefringence $\Delta n = n_e - n_o = \sqrt{\varepsilon_e} - \sqrt{\varepsilon_o}$—found in LCs. Values of birefringence of the state-of-art LC materials used for technological applications are usually in the range of $0.2 - 0.3$. When lower contrast between "empty" and "full" pixels is used, the gaps between the bands in the band structure essentially shrink and only partial bandgaps (existing for a range of wavevectors) are observed instead of full ones. Additionally, if the effect of "empty" and "full" is to be achieved by reorienting the direction of the optical axis of birefringent LC, sharp boundaries between the regions are desired.

To experimentally realize 2D reconfigurable pixelated photonic crystal by using LCs, we suggest the use of dielectric shield walls, as reported in ref.[32] Using such setup allows for driving the voltage and reorienting LC in each individual pixel separately, without leakage of the electromagnetic field. The size of individually driven pixels separated by dielectric walls can be as small as 1 μm.[32] To demonstrate the optical features of such system, we calculated the band diagram, using the refractive indices of 5CB LC ($n_o^2 = \varepsilon_o = 2.25$, $n_e^2 = \varepsilon_e = 3.24$), which are comparable to the refractive indices of LCs in the THz regime[33] and dielectric walls with $\varepsilon_{\text{wall}} = 3$. For the demonstration, we selected a pixelated unit cell with $D = 2$, which is shown in **Figure 5**a. The thickness of the walls is $0.2D$, which corresponds to wall thickness of 200 nm and pixel size of 1 μm, as reported in ref. [32]. Consequently, the size of the unit cell is $A = 4$ μm. Note that we assume sharp change of the refractive index between pixels, whereas experimentally, possibly, the actual realized profile of such change could lead to scattering or coupling of TE and TM modes and would need to be optimized for actual application. The corresponding band diagram is shown in Figure 5b. A partial bandgap with the gap-to-midgap ratio of 0.06 occurs at the M point and has the midgap frequency of $0.423c/A$, corresponding to the wavelength of ≈ 10 μm. Figure 5c,d shows how the band diagram would change for a different distribution of "empty" and "full" pixels within the unit cell. In this particular case, nontrivial photonic effects occur for propagation with k-vector pointing along the diagonal of the unit cell (M-Γ high symmetry points on the band diagram).

While presence of the partial bandgap confirms that LCs can in fact be used to create 2D pixelated photonic crystals with nontrivial optical properties, full bandgaps are usually desired. Larger bandgaps can be achieved by increasing the birefringence of the LCs. Additionally, higher dielectric contrast is also needed for realizing full 3D photonic bandgaps.[1] High birefringence LCs, for example, with Δn up to 0.7, have already been reported.[34–37] Birefringence in THz regime can be also improved by using LC nanoparticle composites.[38,39] With the increased interest in THz spectral range for 6 G wireless communication,[40] also in combination with LCs for the design of active devices,[41] we expect that new and better materials will emerge in the future. By using high birefringence materials or composite materials, self-assembled 2D LC structures with smaller dimensions[42,43] could serve as photonic crystals as well, possibly leading to manipulation of shorter light wavelengths. It is also worth mentioning that only a very simple photonic crystal unit cell has been used in this work as a proof of concept. Therefore, we expect that larger and full bandgaps could also be achieved by further optimizing the configuration of "empty" and "full" pixels or by including insertions (i.e., static pixels) made of materials with higher refractive indices.

3. Conclusion

To conclude, we have shown that the pixelation of the dielectric features within the unit cell of photonic crystals does not have a significant impact on the band structure. Already a low-resolution pixelation which only roughly matches the original structure turns out to be a good approximation for the frequencies of the lowest photonic bands. This shows that pixelated unit

© 2023 The Authors. Advanced Photonics Research published by Wiley-VCH GmbH

cells could be used to simplify the design of photonic crystals. Additionally, the bandgaps are still present in the system even if the contrast in dielectric constants between the pillar and its surrounding is small, namely, comparable to the difference between the ordinary and extraordinary refractive indices in some of the soft birefringent materials. Using those in combination with pixelated design could lead toward fully reconfigurable photonic crystals.

Acknowledgements

This study is part of a project that has received funding from the European Research Council (ERC) under the European Union's Horizon 2020 Research and Innovation Program (Grant agreement No. 884928-LOGOS). The authors also acknowledge funding from Slovenian research agency grants P1-0099, N1-0195 and J1-2462.

Conflict of Interest

The authors declare no conflict of interest.

Data Availability Statement

The data that support the findings of this study are available from the corresponding author upon reasonable request.

Keywords

liquid crystals, photonic crystals, pixels

Received: March 1, 2023
Revised: May 10, 2023
Published online:

[1] J. D. Joannopoulos, S. G. Johnson, J. N. Winn, R. D. Meade, *Photonic Crystals*, Princeton University Press, Princeton, USA and Oxford, UK **2011**.
[2] P. Yeh, M. Hendry, *Phys. Today* **1990**, *43*, 77.
[3] H. Mguez, C. López, F. Meseguer, A. Blanco, L. Vázquez, R. Mayoral, M. Ocaña, V. Fornés, A. Mifsud, *Appl. Phys. Lett.* **1997**, *71*, 1148.
[4] L. Lu, L. Fu, J. D. Joannopoulos, M. Soljačić, *Nat. Photonics* **2013**, *7*, 294.
[5] C. M. Soukoulis, *Photonic Band Gaps and Localization*, NATO Science Series B, volume *308*, Springer Science & Business Media, Berlin, Heidelberg, Germany **2013**.
[6] L. H. Frandsen, A. V. Lavrinenko, J. Fage-Pedersen, P. I. Borel, *Opt. Express* **2006**, *14*, 9444.
[7]] M. Lončar, T. Yoshie, A. Scherer, P. Gogna, Y. Qiu, *Appl. Phys. Lett.* **2002**, *81*, 2680.
[8] L.-H. Wu, X. Hu, *Phys. Rev. Lett.* **2015**, *114*, 223901.
[9] H. Takeda, K. Yoshino, *Phys. Rev. B* **2003**, *67*, 073106.
[10] M. W. Haakestad, T. T. Alkeskjold, M. D. Nielsen, L. Scolari, J. Riishede, H. Engan, A. Bjarklev, *IEEE Photonics Technol. Lett.* **2005**, *17*, 819.
[11] C. Grillet, C. Monat, C. L. Smith, M. W. Lee, S. Tomljenovic-Hanic, C. Karnutsch, B. J. Eggleton, *Laser Photonics Rev.* **2010**, *4*, 192.
[12] M. I. Shalaev, S. Desnavi, W. Walasik, N. M. Litchinitser, *New J. Phys.* **2018**, *20*, 023040.
[13] M. I. Shalaev, W. Walasik, N. M. Litchinitser, *Optica* **2019**, *6*, 839.
[14] R. Rajasekar, G. T. Raja, S. Robinson, *IEEE Trans. Nanotechnol.* **2020**, *19*, 545.
[15] A. Figotin, Y. A. Godin, I. Vitebsky, *Phys. Rev. B* **1998**, *57*, 2841.
[16] F. F. Schlich, P. Zalden, A. M. Lindenberg, R. Spolenak, *ACS Photonics* **2015**, *2*, 178.
[17] V. Schnabel, R. Spolenak, M. Doebeli, H. Galinski, *Adv. Opt. Mater.* **2018**, *6*, 1800656.
[18] W. Park, J.-B. Lee, *Appl. Phys. Lett.* **2004**, *85*, 4845.
[19] S. Kim, V. Gopalan, *Appl. Phys. Lett.* **2001**, *78*, 3015.
[20] Y. Huang, Y. Zhou, C. Doyle, S.-T. Wu, *Opt. Express* **2006**, *14*, 1236.
[21] L. Rossi, P. Fischer, T. Rohe, N. Wermes, *Pixel Detectors: From Fundamentals to Applications*, Springer Science & Business Media, **2006**.
[22] A. Tittl, A. Leitis, M. Liu, F. Yesilkoy, D.-Y. Choi, D. N. Neshev, Y. S. Kivshar, H. Altug, *Science* **2018**, *360*, 1105.
[23] L. Hu, L. Xuan, Y. Liu, Z. Cao, D. Li, Q. Mu, *Opt. Express* **2004**, *12*, 6403.
[24] A. S. Ostrovsky, C. Rickenstorff-Parrao, V. Arrizón, *Opt. Lett.* **2013**, *38*, 534.
[25] G. Lazarev, A. Hermerschmidt, S. Krüger, S. Osten, *Opt. Imaging Metrol.: Adv. Technol.* **2012**, *1*, 29.
[26] Z. Zhang, Z. You, D. Chu, *Light: Sci. Appl.* **2014**, *3*, e213.
[27] W. Choi, S.-H. Kim, J. Jang, J.-K. Park, *Microfluid. Nanofluid.* **2007**, *3*, 217.
[28] H. Quan, T. Zhang, H. Xu, S. Luo, J. Nie, X. Zhu, *Bioact. Mater.* **2020**, *5*, 110.
[29] M. Mele, G. Campana, G. Fumelli, *Sust. Prod. Consumption* **2021**, *28*, 405.
[30] C. J. R. Sheppard, *Appl. Opt.* **2018**, *57*, 7878.
[31] S. G. Johnson, J. D. Joannopoulos, *Opt. Express* **2001**, *8*, 173.
[32] Y. Isomae, T. Ishinabe, Y. Shibata, H. Fujikake, *J. Soc. Inf. Disp.* **2019**, *27*, 251.
[33] X. Li, N. Tan, M. Pivnenko, J. Sibik, J. A. Zeitler, D. Chu, *Liq. Cryst.* **2016**, *43*, 955.
[34] R. Dabrowski, P. Kula, J. Herman, *Crystals* **2013**, *3*, 443.
[35] S. Gauza, C.-H. Wen, S.-T. Wu, N. Janarthanan, C.-S. Hsu, *Jpn. J. Appl. Phys.* **2004**, *43*, 7634.
[36] Y. Arakawa, S. Kang, H. Tsuji, J. Watanabe, G.-i. Konishi, *RSC Adv.* **2016**, *6*, 92845.
[37] J. Herman, P. Kula, *Liq. Cryst.* **2017**, *44*, 1462.
[38] E. Mavrona, U. Chodorow, M. Barnes, J. Parka, N. Palka, S. Saitzek, J.-F. Blach, V. Apostolopoulos, M. Kaczmarek, *AIP Adv.* **2015**, *5*, 077143.
[39] U. Chodorow, E. Mavrona, N. Palka, O. Strzezysz, K. Garbat, S. Saitzek, J.-F. Blach, V. Apostolopoulos, M. Kaczmarek, J. Parka, *Liq. Cryst.* **2017**, *44*, 1207.
[40] T. S. Rappaport, Y. Xing, O. Kanhere, S. Ju, A. Madanayake, S. Mandal, A. Alkhateeb, G. C. Trichopoulos, *IEEE Access* **2019**, *7*, 78729.
[41] H. Yu, H. Wang, Q. Wang, S. Ge, W. Hu, *App. Sci.* **2023**, *13*, 1428.
[42] J.-i. Fukuda, S. Žumer, *Nat. Commun.* **2011**, *2*, 246.
[43] G. Poy, A. J. Hess, A. J. Seracuse, M. Paul, S. Žumer, I. I. Smalyukh, *Nat. Photonics* **2022**, *16*, 454.

© 2023 The Authors. Advanced Photonics Research published by Wiley-VCH GmbH